Superconductivity in alkaline earth metal doped boron hydrides

Wen-Hua Yang,[*,1] Wen-Cai Lu,[*,1,2] Shan-Dong Li,[1] Xu-Yan Xue,[1] Wei Qin,[1]

[1]College of Physics and Laboratory of Fiber Materials and Modern Textile, Growing Base for State Key Laboratory, Qingdao University, Qingdao, Shandong 266071, P. R. China

[2]Institute of Theoretical Chemistry, Jilin University, Changchun, Jilin 130021, P. R. China

K. M. Ho[3] and C. Z. Wang[3]

[3]Ames Laboratory-U.S. DOE and Department of Physics and Astronomy, Iowa State University, Ames, IA 50011, U.S.A

ABSTRACT

Effects of alkaline earth metal atoms doping in boron hydrides at high pressure are investigated by first-principles calculations. The calculated results showed that doping with Mg, Ca, Ba, and Sr in B_8H_{16} at 50 GPa is thermodynamically favorable and dynamically stable. The doping changes the B_8H_{16} from a semiconductor to a metal with substantial electronic density-of-state around the Fermi level. The superconductivity of the alkaline earth metal doped B_8H_{16} is studied based on electron-phonon coupling mechanism. The calculated critical superconducting transition temperatures (T_c) range from 10 to 25 K at 50 GPa upon doping. These results suggest that doping metal atoms in boron hydrides is an efficient way in designing superconducting materials.

---

[*]Corresponding author. Email: yangwh@qdu.edu.cn; wencailu@jlu.edu.cn

1. Introduction

Recently, hydrogen-rich compounds have received considerable attention due to their potential high-temperature superconductivity at high pressure [1-4]. Pressure can induce novel physical and chemical properties in materials because the reduction of interatomic distance under pressure can strengthen the chemical bonding between the atoms and lead to stabilization of new structures which are very different from the ground-state of the materials at ambient pressure. Extensive experimental and theoretical investigations have been performed to explore the superconductivity of hydride compounds under high pressure [1-12]. For example, binary hydrides (e.g., CaH_6, MgH_6, AsH_8, GeH_3, Si_2H_6, TaH_6, and BH_3, and so on) have been shown to have possible superconductivity at high-T_c of 100 -280 K in the pressure range of 140-300 GPa [5-12]. Recently, it has been reported by experimental study that the superconducting T_c of sulfur hydrides can reach 203 K at 155 GPa, which confirmed the theoretical prediction that the T_c of H_3S is 191–204 K at 200 GPa [1,2]. For ternary hydrides, the T_c of the Cmc21 structure of Fe_2SH_3 was predicted to be 0.30 K at 173 GPa [13]. The ternary hydrides Mg-Si-H and Mg-Ge-H as potential superconductors were systematically investigated by Ma *et al* [14,15]. They showed that the T_c value of $MgSiH_6$ and $MaGeH_6$ are ~63 K at 250 GPa, and ~67 K at 200 GPa, respectively. Moreover, $CaYH_{12}$ with Fd-3m symmetry [16] is predicted to be have T_c is 258 K at 200 GPa. The compound is stable above 170 GPa, which not only remains hydrogen-clathrate as CaH_6 and YH_6, but also is energetically favored relative to CaH_6 and YH_6 at 200 GPa. Experimentally, more and more ternary systems

(i. e., $BaReH_9$, Li_5MoH_{11}, La-H, C-S-H) were the successfully synthesized [3,4,17,18], which showed superconductivity under high pressure. Particularly, the recent experiment discovery of record high temperature superconductivity (T_c ~ 287 K at 267 GPa) in C-S-H compounds is an important advance toward room temperature superconductors [4].

It has been shown that proper doping is one of the effective ways to enhance the superconductor properties. For example, by substituting half of the bromine atoms in the P4/nmm HBr at 170 GPa, the T_c can increase from 73 K in P4/nmm HBr to 95 K in P4mm $HCl_{0.5}Br_{0.5}$ [19]. It has also been pointed out that lower mass, higher coordination number, shorter bonds, and more highly symmetric environment for hydrogen atoms are important to enhance the superconducting property of hydrides [19]. For sulfur hydrogen systems, O-doped and P-doped can promote the ionic character so that the T_c values can be improved, and T_c ~280 K at 250 GPa for $H_3S_{0.925}P_{0.075}$ has been reported [20]. By doping Mg into CH_4, the P4/nmm-$MgCH_4$ becomes a good superconductor with a T_c of 84~121 K in the pressure range of 75~120 GPa [21]. The superconductivity and structures of gold hydrides with pressure were also systematically investigated [22]. It is interesting to note that while gold hydrides are not stable below 300 GPa, $AE(AuH_2)_2$ (AE=Ba and Sr) formed by Ba or Sr doping were predicted to be thermodynamically stable and exhibit superconductivity with T_c of 30 K and 10 K at 1atm, repetitively.

As one of the lightest materials, boron hydrides also have received a lot of attentions. The superconducting T_c of the layered P_6/mmm-BH structure is ~21 K at

175 GPa [23]. The Pbcn-B_2H_6 becomes a stable phase above 350 GPa, and its T_c can be as high as 125 K at 360 GPa [12]. Recently, we systematically investigated the crystal structures of BH_2 under high pressures [24]. The calculated results showed that the C2/c-BH_2 has T_c of ~38 K at 250 GPa. The calculated results also showed that the Cmcm-BH_2 has the lowest formation enthalpy at 50 GPa, but it has a small energy gap (0.13 eV) around the Fermi level thus lack of superconductivity. An interesting question naturally arisen is whether the electronic structure at the Fermi level in this structure can be manipulated through metal doping such that superconductivity of the compound can be enhanced.

In this paper, we design alkaline earth metal doped MB_8H_{16} compounds with M being Be, Mg, Ca, Sr and Ba, and investigate the structure stability, electron-phonon coupling properties and possible superconductivity of the doped compounds at 50 GPa. We show that by contrast to the Cmcm-B_8H_{16} phase which has a small energy gap [24], Ca and Mg doped B_8H_{16}(i.e., CaB_8H_{16} and MgB_8H_{16}) exhibit substantial electronic DOS at the Fermi level and become good superconductors with T_c ~20 K at 50 GPa.

2. Computational methods

The DFT calculations for structure optimizations energies, and band structures are performed using the ultrasoft pseudopotentials (USP) [25] and the codes in the Cambridge Serial Total Energy Package (CASTEP) [26]. The generalized gradient approximation (GGA) using Perdew-Burke-Ernzerhof (PBE) [27] functional was adopted to treat the exchange and correlation energy. The electron wave functions

were expanded by a basis set of plane waves with an energy cutoff of 1000 eV. Appropriate Monkhorst-Pack Brillouin sampling grid of spacing $2\pi \times 0.02$ A^{-1} were used for all cases. The convergence criterion is 0.02 meV/atom for the total energy and 0.05 eV/Å for the forces on the atoms. The phonon spectrum and electron-phonon coupling calculations (EPC) were performed using the Quantum-ESPRESSO package [28]. Ultrasoft pseudopotentials with a cutoff of 80 Ry were adopted for the QE calculations. The EPC parameter was calculated using 16×16×4 k-point and 4×4×1 q-point meshes for MgB_8H_{16} and CaB_8H_{16}. The superconducting T_c was estimated using Allen-Dynes modified McMillan equation [29]:

$$T_c = \frac{\hbar}{k_B}\frac{\omega_{\log}}{1.20}\exp\left[\frac{-1.04(1+\lambda)}{\lambda(1-0.62\mu^*)-\mu^*}\right] \quad (1)$$

where $\hbar$ is the reduced Planck constant, k_B is the Boltzmann constant (here $\hbar$ and k_B are in the natural units), λ is electron-phonon coupling parameter, $\omega_{\log}$ is the logarithmic average phonon frequency , and μ is the Coulomb pseudopotential representing Coulombic repulsion, for which we used the value of 0.10 ~ 0.13. The EPC constant and $\omega_{\log}$ were calculated as:

$$\lambda = 2\int_0^\infty \frac{\alpha^2 F(\omega)}{\omega} d\omega \quad (2)$$

and

$$\omega_{\log} = \exp\left[\frac{2}{\lambda}\int \frac{d\omega}{\omega}\alpha^2 F(\omega)\ln(\omega)\right] \quad (3)$$

3. Results and discussion

The Cmcm-BH_2 (the crystallographic details are given in the supplementary material) at 50 GPa obtained from our previous study [24] can be viewed as a periodic stacking of a $(BH)_2$ slab and a H_2 lattice layer as shown in Fig. 1 (a) and (b). The B atoms in the $(BH)_2$ slab form a buckled hexagonal layer and each B atom has six B neighbors. The buckled B layer is passivated by H to form the slab between the H_2 lattice layers. For alkaline earth metal doped MB_8H_{16} structures, we tried a variety of insertion ways, as shown in Fig.S1. We found that alkaline earth metal atom inserted into the hole formed by the buckled B layer and the passivated H atoms has the lowest energy (Table S2). The structures of the MgB_8H_{16} and CaB_8H_{16} compounds after the relaxation are shown in Fig. 1 (d) and (e). We can see that the lattice is distorted by the metal atom insertion. After the insertion of alkaline earth metal atoms, the H_2 originally with H-H bond length of 0.739 Å in the hydrogen layer is also separated into two H atoms (with H-H distance changes to 1.999 Å). The high symmetry of the original structure is destroyed, and the volume expansion is about 4.26-22.87%.

The formation enthalpy of the metal inserted compounds after the relaxation at 50 GPa is calculated to assess the energetic stability of MB_8H_{16}. The formation enthalpy is defined as

$$\Delta H_f = \left[H(M_xB_yH_z) - yH(B) - zH(H) - xH(M) \right] / (x+y+z) \qquad (4)$$

Here ΔH_f is the enthalpy of formation per atom, H indicates the enthalpy of each related compound. The calculated formation enthalpy of different metal-inserted structures are plotted Fig. 2. The results showed that all the alkaline earth metal doped

structures have negative formation enthalpy, except Be-doped structure. These results indicates that expect Be, other alkaline earth metal insertion is energetically favorable.

Alkaline earth metal atoms insertion not only stabilize the structures, but also affect the electronic properties. In order to investigate the effect of the chemical precompression induced by alkaline earth metal atoms, we compared the electronic band structure and density-of-state of Cmcm-B_8H_{16} with those of MgB_8H_{16} and CaB_8H_{16}. The band structures along the high-symmetry lines G-F-Q-Z-G are shown in Fig. 3, respectively. The Cmcm-B_8H_{16} is a semiconductor with a band gap of about 0.13 eV. The valence band and conduction bands close to the Fermi level are dominated by boron *p* state. For the alkaline earth metal doped systems, the Fermi level moves up into the conduction bands due to the increase of electron density, which transfers the semiconductor into a metal. The Bader charge analysis was performed to calculate to the transferred electrons for the MgB_8H_{16} and CaB_8H_{16} compounds. The charge transfer from Mg and Ca atom to the Cmcm-B_8H_{16} is about 2.21 e and 1.06 e, respectively. We also analyzed the electronic density-of-states (DOS) and observed that alkaline earth metal atom doping enhance the DOS at the Fermi level. As one can see from Fig. 3, Mg and Ca doping in Cmcm-B_8H_{16} introduces some flat bands around the Fermi level thus greatly enhance the electronic DOS around the Fermi energy, which indicates a good metallic behavior.

The calculated phonon dispersions and phonon DOS for B_8H_{16} and Mg/Ca-doped B_8H_{16} are shown in Fig. 4 and Fig. 5 respectively. Note the Cmcm-B_8H_{16} is not dynamically stable at 50 GPa, which has some imaginary

frequency in the phonon dispersion. The imaginary modes are mainly from the H_2 unites. While for the Mg/Ca doped B_8H_{16}, no imaginary frequencies in the phonon spectra are observed, indicating the doped structures are also dynamically stable.

For conventional superconductivity, electron pairing (i.e., formation of Cooper pairs) mechanism is phonon mediated and electron phonon coupling plays an important role. In addition to modify the electron density, metal doping would also be important for increasing the electron phonon coupling constant λ to enhance the superconductivity. For example, Li-intercalated phosphorene were predicted to exhibit superconductivity with a T_c about ~15 K [30]. Ca-intercalated bilayer grapheme [31] with a T_c about 7 K. We also explore the possible superconductivity in the metal-doped boron hydride compound B_8H_{16}. The logarithmic average phonon frequency $\omega_{\log}$, the electron-phonon coupling (EPC) parameter λ, and the electronic DOS at the Fermi level, $N(E_f)$, are calculated and summarized in Table I. For the MgB_8H_{16} (or CaB_8H_{16}) at 50 GPa, the calculated results show that λ, and $\omega_{\log}$ reaches 1.22 (0.60), and 268 (599) K, respectively. The metal doping also introduces large $N(E_f)$ with 6.9 and 5.0 states/Ry for MgB_8H_{16} and CaB_8H_{16} at 50 GPa, respectively. According to the Allen-Aynes modified McMillan formula [29] and taking the typical Coulomb pseudopotential parameters, $\mu =$ 0.10~0.13, the superconducting T_c is estimated to be 22-25 K and 10-14 K for MgB_8H_{16} and CaB_8H_{16} at 50 GPa, respectively.

For MgB_8H_{16} (Fig. 5), the low frequency (< 8 THz) phonon bands formed by three acoustic branches are mainly coming from the vibrations of Mg atom, which

contribute 60% of the total λ. The middle frequency (8-33 THz) are primarily related to the B and H atoms, and with small contribution of Mg atom. This frequency range contributes 37% of λ. The high frequency vibration (> 33 THz) modes from the H atoms only contribute 3% of the total λ. For CaB_8H_{16} (Fig. 5), the low frequency (< 6 THz) and high frequency (> 33 THz) vibrations are dominated by the H atoms and contribute 15% of the total λ. The contribution from the medium frequency range of B and H atoms is 49% of total λ. Interestingly, we noted that there are two peaks located at about 8 THz and 10 THz in the phonon DOS of Ca atom, which contribute 36% of λ. Thus, the vibration of metal atoms plays an important role in the electron phonon coupling in these systems. We have also calculated the phonon spectra and electron-phonon coupling in Ba and Sr doped B_8H_{16}. The results show that the BaB_8H_{16} and SrB_8H_{16} are also dynamically stable at 50 GPa (see Fig. S2-S4 in the supporting materials). The superconducting T_c is estimated to be 20-25 K for BaB_8H_{16} and 12-16 K for SrB_8H_{16}. These results suggest that doping metal atoms in boron hydrides is an efficient way in designing superconducting materials.

4. Conclusion

In summary, we investigated the stability and superconductivity of B_8H_{16} with doping by alkaline earth metal atom M (M=Be, Mg, Ca, Sr, and Ba). The results from first-principles DFT calculations showed that the doping is thermodynamically favorable and dynamically stable expect Be doping. Upon doping, the system changes

from a semiconductor to a metallic phase and the $N(E_f)$ increases substantially due to the flat bands around the Fermi level induced by the doping. The alkaline earth metal doping in the Cmcm-B_8H_{16} structure also turns the compound into a good superconductor. Electron-phonon coupling calculations reveal that the T_c of MgB_8H_{16} is about ~20 K at 50 GPa. Our study suggests that doping metal atoms in boron hydrides would an efficient way to manipulate the superconductivity of the materials.

Credit author statement

Wenhua Yang: Data curation, Writing-Original draft preparation, Reviewing and Editing. Wencai Lu: Writing-Reviewing and Editing, Supervision. Shandong Li: Investigation. Xuyan Xue: Investigation. Wei Qin: Investigation. K. M. Ho: Reviewing and Editing. C. Z. Wang: Reviewing and Editing.

Declaration of competing interest

The authors declare that they have no known competing financial interests or personal relationships that could have appeared to influence the work reported in this paper.

Appendix A. Supplementart material

See the supplementary material for the crystallographic data of Cmcm-B_8H_{16}; the formation enthalpies for the alkaline earth metal atom inserted Cmcm-B_8H_{16}; electronic band structures and density of states of MB_8H_{16} (M=Be, Sr and Ba) at 50 GPa; phonon band structures of SrB_8H_{16} and BaB_8H_{16} at 50 GPa.

Acknowledgments

This work was supported by the National Natural Science Foundation of China (Grant No. 21773132 and No. 21603114); Natural Science Foundation of Shandong Province (Grant no. ZR2020MB046); the Higher Educational Science and Technology Program of Shandong Province of China (Grant No. J17KA179); the Project funded by the Qingdao Postdoctoral Application Research Project (Grant No. 2016008). This work was also supported by the U.S. Department of Energy (DOE), Office of Science, Basic Energy Sciences, Materials Science and Engineering Division including a grant of computer time at the National Energy Research Scientific Computing Centre (NERSC) in Berkeley, CA. Ames Laboratory is operated for the U.S. DOE by Iowa State University under contract # DE-AC02-07CH11358.

References

[1] A. P. Drozdov, M. I. Eremets, I. A. Troyan, V. Ksenofontov and S. I. Shylin, Nature, 525 (2015) 73.

[2] D. F. Duan, Y. X. Liu, F. B. Tian, D. Li, X. L. Huang, Z. L. Zhao, H. Y. Yu, B. B. Liu, W. J. Tian and T. Cui, Sci Rep, 4 (2014) 6968.

[3] M. Somayazulu, M. Ahart, A. K. Mishra, Z. M. Geballe, M. Baldini, Y. Meng, V. V. Struzhkin, and R. J. Hemley, Phys. Rev. Lett., 122 (2019) 027001.

[4] S. Elliot, D. G. Nathan, M. Raymond, D. Mathew, V. Hiranya, V. Kevin, V. L. Keith, S. Ashkan and P. D. Ranga. Nature, 586 (2020) 373 .

[5] X. Feng, J. Zhang, G. Gao, H. Liu, and H. Wang, RSC Adv, 5 (2015) 59292.

[6] H.Wang, J. S. Tse, K. Tanaka, T. Iitaka and Y. Ma, Proc. Natl. Acad. Sci. U. S. A., 109 (2012) 6463.

[7] Y F. Ge, F. Zhang, and Y. G. Yao, Phys. Rev. B., 93 (2016) 224513.

[8] Y. H. Fu, X. P. Du, L. J. Zhang, F. Peng, Chem. Mater., 28 (2016) 1746.

[9] K. Abe and N. W. Ashcroft, Phys. Rev. B., 88 (2013) 174110.

[10] X. L. Jin, X. Meng, Z. He, Y. M. Ma, B. B. Liu, T. Cui. G. T. Zou, and H. K. Mao, Proc. Natl. Acad. Sci. U.S.A.,107 (2010) 9969.

[11] Q. Zhuang, X. L. Jin, T. Cui, Y. B. Ma, Q. Q. Lv, Y. Li, H. Zhang, H. D. Zhang, X. Meng, and K. Bao, Inorg. Chem. 56 (2017) 3901.

[12] K. Abe and N. W. Ashcroft, Phys. Rev. B., 84 (2011)104118.

[13] S. Zhang, L. Zhu, H. Liu, and G. Yang, Inorg. Chem., 55 (2016) 11434 .

[14] Y. Ma, D. Duan, Z. Shao, H. Yu, H. Liu, F. Tian, X. Huang, D. Li, B. Liu, and T. Cui, Phys. Rev. B., 96 (2017) 144518.

[15] Y. Ma, D. Duan, Z. Shao, D. Li, L. Wang, H. Yu, F. Tian, H. Xie, B. Liu, and T. Cui, Phys. Chem. Chem. Phys. 19 (2017) 27406.

[16] X. W. Liang, A. Bergara, L. Y. Wang, B. Wen, Z. S. Zhao, X. F. Zhou, J. L. He, G. Y. Gao, and Y. J. Tian, Phys. Rev. B., 99 (2019) 100505.

[17] T. Muramatsu, W. K. Wanene, M. Somayazulu, E. Vinitsky,D. Chandra, T. A. Strobel, V. V. truzhkin and R. J. Hemley, J. Phys. Chem. C., 119 (2015) 18007.

[18] Z. M. Geballe, H. Liu, A. K.Mishra, M. Ahart, M. Somayazulu,Y. Meng, M. Baldini, and R. J. Hemley, Angew. Chem., Int. Ed. 57 (2018) 688.

[19] Q. Gu, P. Lu, K. Xia, J. Sun, D. Xing, Phys. Rev. B., 6 (2017) 064517.

[20] C. Heil and L. Boeri, Phys. Rev. B., 92 (2015) 060508.

[21] F. Tian, D. Li, D. Duan,X. Sha, Y. Liu, T. Yang, B. Liu and T. Cui, Mater. Res. Express., 2 (2015) 046001.

[22] M. Rahm, R. Hoffmann, and N. W. Ashcroft, J. Am. Chem. Soc., 139 (2017) 8740.

[23] C. H. Hu, A. R. Oganov, Q. Zhu, G. R. Qian, G. Frapper, A. O. Lyakhov, and H. Y. Zhou, Phys. Rev. Lett., 110 (2013) 165504.

[24] W. H. Yang，W. C. Lu，S. D. Li, X. Y. Xue, Q. J. Zang, K. M. Ho and C. Z. Wang，Phys. Chem. Chem. Phys., 21 (2019) 5466.

[25] D. Vanderbilt, Phys. Rev. B., 41 (1990) 7892.

[26] V. Milman, B. Winkler, J. A. White, C. J. Pickard, M. C. Payne, E. V. Akhmatskaya, and R. H. Nobes, Int. J. Quantum Chem., **77** (2000) 895.

[27] J. P. Perdew, K. Burke, and M. Ernzerhof, Phys. Rev. Lett., 77 (1996) 3865.

[28] P. Giannozzi, S. Baroni, N. Bonini, M. Calandra, R. Car, C. Cavazzoni, G. L. Chiarotti, M. Cococcioni, I. Dabo, A. Dal Corso, *et al* .J. Phys.: Condens. Matter, 21 (2009) 395502.

[29] P. B. Allen and R. C. Dynes, Phys. Rev. B.,12 (1975) 905.

[30] G. Q. Huang, Z. W. Xing, and D. Y. Xing, Appl. Phys. Lett. 106 (2015)113107.

[31] E. R. Margine, H. Lambert and F. Giustino, Sci Rep., 6 (2016) 21414.

Table 1 Calculated λ, ω_{log}, N(E_f) and T_c of MB_8H_{16} (M=Mg, Ca, Sr and Ba) at 50 GPa; $N(E_f)$ is the DOS at Fermi level, in states/Ry; ω_{log} and T_c's are in K.

Structure	Pressure (GPa)	λ	$N(E_f)$	ω_{log}	T_c μ =0.10	T_c μ =0.13
MgB_8H_{16}	50	1.22	6.9	268	25	22
CaB_8H_{16}	50	0.60	5.0	599	14	10
SrB_8H_{16}	50	0.75	12.5	616	25	20
BaB_8H_{16}	50	0.72	10.7	416	16	12

Figure captions

Fig. 1. Structures of Cmcm-B_8H_{16} and Mg/CaB_8H_{16} at 50 GPa. (a) and (b) Cmcm-B_8H_{16}. (c) The initial structure with M doping (M=Mg, Ca, Ba, and Sr) before relaxation. (d) and (e) The optimized structures of MgB_8H_{16} and CaB_8H_{16}. The green, pink, blue and purple spheres represent the B, H, Mg and Ca atom, respectively.

Fig. 2. Formation enthalpies of MB_8H_{16} (M=Be、Mg、Ca、Sr and Ba) at 50 GPa.

Fig. 3. Electronic band structures and partial density of states for Cmcm-B_8H_{16} and Mg/CaB_8H_{16} structures at 50 GPa. (a) Cmcm-B_8H_{16}. (b) MgB_8H_{16} and (c) CaB_8H_{16}, respectively.

Fig. 4. (a) Calculated phonon band structure for Cmcm-B_8H_{16} at 50 GPa. (b) The projected phone density of states on the B atom and H_2 unites.

Fig. 5. (a) and (d) Calculated phonon band structures for MgB_8H_{16} and CaB_8H_{16} at 50 GPa. (b) and (e) The projected phone density of states on the Mg, Ca, B and H atoms. (c) and (f) The Eliashberg phonon spectral function $\alpha^2F(\omega)$ and the electron-phonon intergral $\lambda(\omega)$ of MgB_8H_{16} and CaB_8H_{16} at 50 GPa.

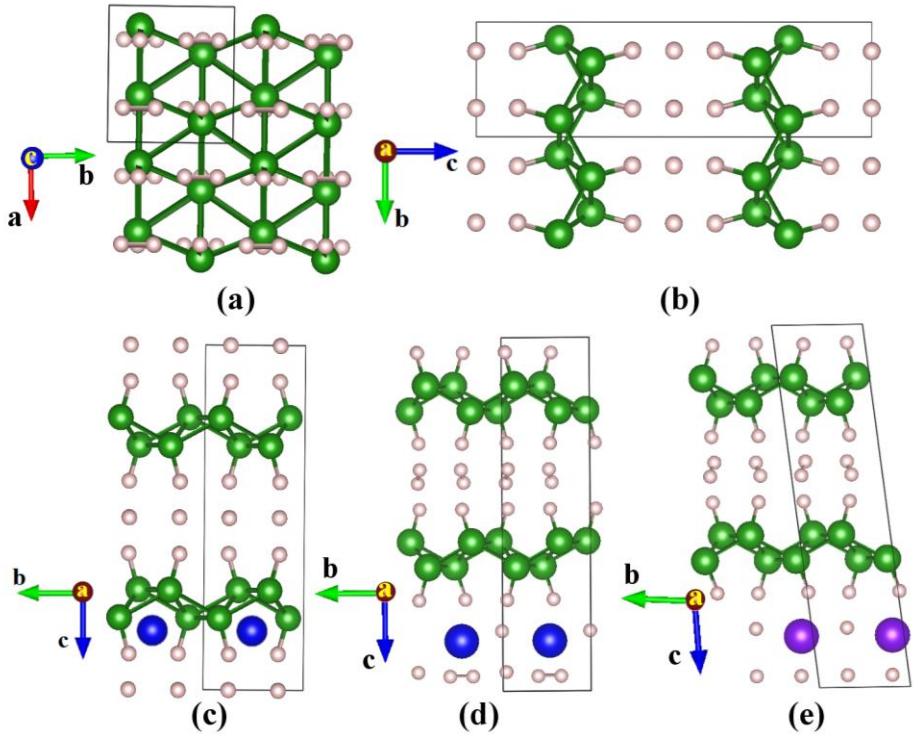

Fig 1. Structures of Cmcm-B_8H_{16} and Mg/CaB_8H_{16} at 50 GPa. (a) and (b) Cmcm-B_8H_{16}. (c) The initial structure with M doping (M=Mg, Ca, Ba, and Sr) before relaxation. (d) and (e) The optimized structures of MgB_8H_{16} and CaB_8H_{16}. The green, pink, blue and purple spheres represent the B, H, Mg and Ca atom, respectively.

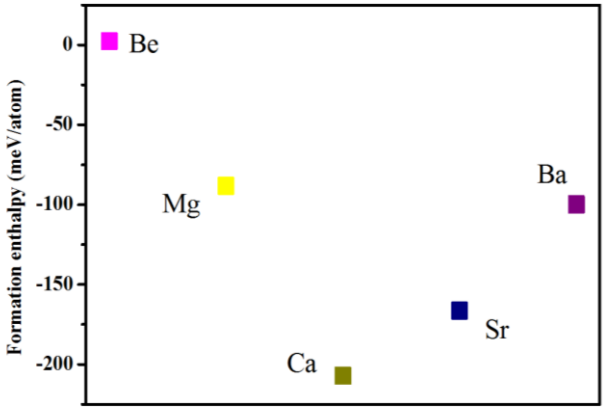

Fig. 2. Formation enthalpies of MB_8H_{16} (M=Be、Mg、Ca、Sr and Ba) at 50 GPa.

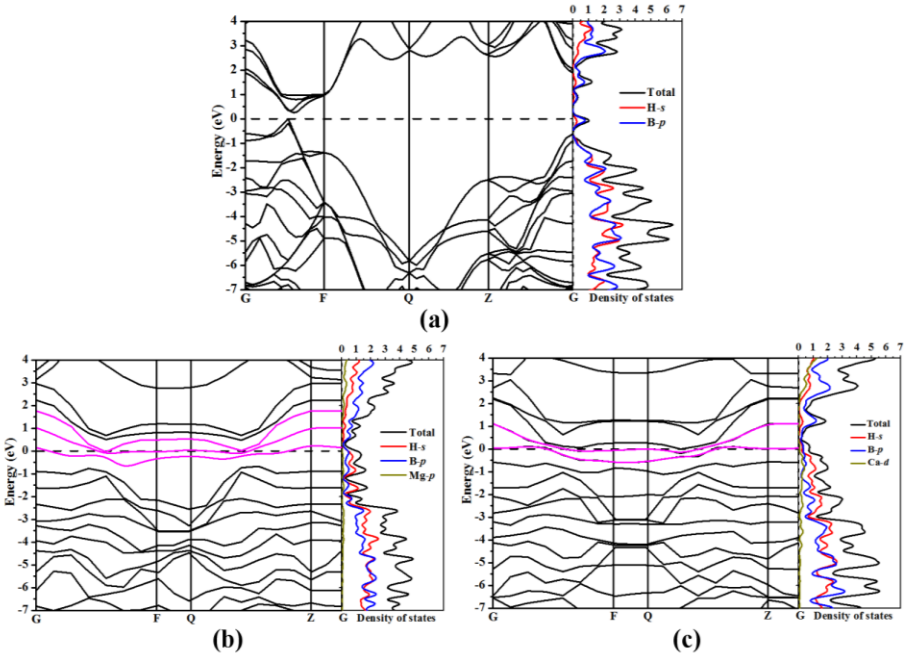

Fig. 3 Electronic band structures and partial density of states for Cmcm-B_8H_{16} and Mg/CaB_8H_{16} structures at 50 GPa. (a) Cmcm-B_8H_{16}. (b) MgB_8H_{16} and (c) $CaB_8H_{16,}$ respectively.

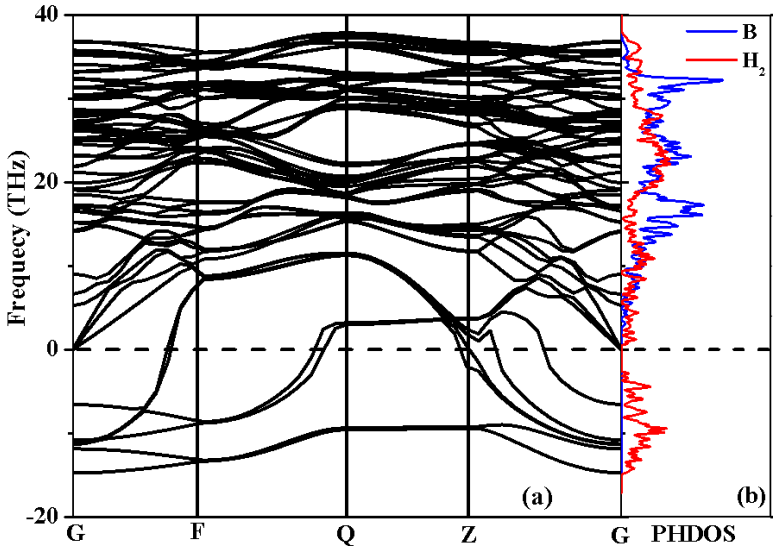

Fig. 4 (a) Calculated phonon band structure for Cmcm-B_8H_{16} at 50 GPa. (b) The projected phone density of states on the B atom and H_2 unites.

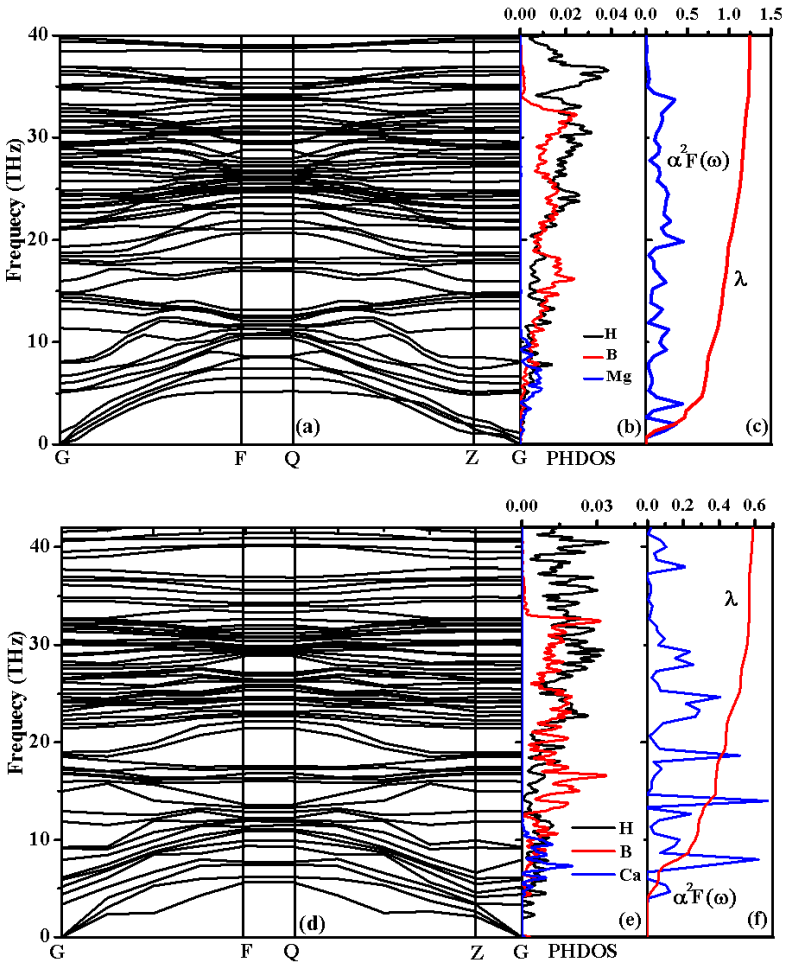

Fig. 5. (a) and (d) Calculated phonon band structures for MgB_8H_{16} and CaB_8H_{16} at 50 GPa. (b) and (e) The projected phone density of states on the Mg, Ca, B and H atoms. (c) and (f) The Eliashberg phonon spectral function, $\alpha^2 F(\omega)$, and the electron-phonon intergral $\lambda(\omega)$ of MgB_8H_{16} and CaB_8H_{16} at 50 GPa.